Two Stage PV Generation System with Control Strategy to Improve Grid Integrating Capabilities During Partial Shading Conditions

S. Keerthi Sonam *†, R. Balamurugan **, Karuppiah Natarajan ***

*†Research Scholar, Department of Electrical and Electronics Engineering, Annamalai University, Annamalai Nagar (608 002), Tamilnadu, India.

**Associate Professor, Department of Electrical Engineering, Annamalai University, Annamalai Nagar (608 002), Tamilnadu, India.

***Department of Electrical and Electronics Engineering, Vardhaman College of Engineering, Hyderabad (501 218), Telangana, India

(keerthi06210@gmail.com, bala_aucdm@yahoo.com, natarajankaruppiah@gmail.com)

† S. Keerthi Sonam; Department of Electrical and Electronics Engineering, Annamalai University, Annamalai Nagar (608 002), Tamilnadu, India, Tel: +9701746514

Received: 06.07.2023 Accepted:08.08.2023

Abstract- The presented work introduces a grid-integrated photovoltaic (PV) generation system, that incorporates a DC-to-DC converter and a DC to AC inverter specifically designed to handle partial shading conditions. The DC-to-DC converter employs an MPPT algorithm inspired by the construction of the Giza Pyramid, while the inverter is controlled using virtual synchronous generation (VSG) control. The GPC based MPPT algorithm is used to optimize the PV system's energy harvesting capabilities. By leveraging mathematical principles and optimization techniques inspired by the pyramid's design, the Giza Pyramid construction based MPPT algorithm aims to enhance the description of a synchronous generator. This paper aims to upgrade the overall efficacy of the PV systems, particularly under challenging operating conditions like partial shading conditions. VSG control enables renewable energy systems to seamlessly integrate with the existing power grids. It helps to maintain grid stability during normal operation, handle grid disturbances, and support grid voltage and frequency control. The system simulation is conducted with MATLAB/Simulink. The gained outcomes are assessed with those obtained from a PV system employing a Particle Swarm Optimization (PSO) MPPT process. The comparative analysis provides the effectiveness of the intended MPPT algorithm in handling partial shading situations.

Keywords: Particle Swarm Optimization, virtual synchronous generation control, MPPT, Giza Pyramid Construction Algorithm, DC to DC converter

1. Introduction

The utilization of energy sources by distributed generators (DGs) is increasing nowadays [1]. This trend is attributed to the growing recognition of the negative effect of environmental pollution. The stability of the power system becomes a significant concern. Conventional synchronous generators (SGs) are commonly employed for maintaining the power grid frequency [2]. The inertial response of synchronous generators (SGs) can effectively by regulated either gripping or supplying the kinetic energy stowed in their rotors. Synchronous generators (SGs) show an important role in regulating the frequency response of the power grid [3] resulting in a smoother frequency control. In addition, synchronous generators (SGs) can deliver a significant amount of kinetic energy to sudden disturbances

or Traditional synchronous generators (SGs) have a crucial function in supporting the utility grid [4]. Conversely, distributed generators (DGs) based on inverters lack the essential inertia and grid-forming capability, posing a risk to the strength of the power grid [5]. To address the challenges associated with inverter-based distributed generators (DGs), a control strategy based on virtual synchronous generators was designed. In recent times, multiple algorithms have been developed for virtual synchronous generators (VSGs) [6]. The fundamental principle of VSG control is justified in adopting the widely used swing equation for synchronous generators (SGs) through droop control [7]. Therefore, VSG control emulates the essential attributes of synchronous generators (SGs), such as inertia and droop mechanism, to enable the emulation of rotating inertia in inverter-based distributed generators (DGs). With its inherent capabilities, the VSG has the potential to enhance grid stability.

Furthermore, the control system of the VSG can operate around islanded mode as well, facilitating natural load sharing like traditional synchronous generators (SGs) [8]. Consequently, a significant amount of research has been dedicated to the control of VSGs, as discussed in detail in [9]. In [10], a pioneering approach was presented, with a corrective VSG control structure. The aim of this algorithm is to effectively mitigate distorted current waveforms. In [11], an alternative approach was investigated to enhance synchronization stability. This method utilizes the frequency change among the power grid and the virtual synchronous generator (VSG) is utilized to manage reactive control within the system. Moreover, in the context of microgrid systems equipped with grid-connected inverters of distributed generators (DGs), [12] introduced a specialized virtual synchronous generator (VSG) with a fuzzy secondary controller. This VSG was specifically designed to regulate voltage and frequency.

To tackle the challenges, researchers and academics have made efforts to address them by incorporating the inverter power factor modeling and then integrating rotor swing equations to the inverter control system. This method allows the inverter to drive as a VSG by providing virtual inactivity [13]. Since 2008, various configurations for VSG techniques have been proposed worldwide [14]. These approaches encompass diverse methods such as particle swarm optimization, as recommended in [15], which considers voltage angle deviations of generators; pole placement for oscillation damping, as presented in [16]; a hybrid control method that combines inactivity and checking for islanded microgrids, as explained in [17]; simulated excitation control method [18]; and enhanced fuzzy logic controllers [19], among several others.

In recent times, there have been multiple attempts to alter and adjust droop control techniques. In a study referenced as [20], a novel approach to virtual synchronous generator control was developed, featuring the integration of adaptable droop coefficients. This approach aims to tackle challenges such as less energy allocation and a significant reduction in frequency oscillations in islanded microgrids. The challenges such as reduced power quality and significant frequency oscillations in islanded microgrids, [21] introduced a control technique for virtual synchronous generators created on adaptive droop coefficients. The control approach employed for VSGs exhibited remarkable accuracy in power distribution, this approach results in improved active performance and frequency stability of the power grid system. Furthermore, implementing the same VSG control methodology enables better voltage stability in microgrid systems through voltage deviation adjustments.

Researchers in [22] studied the impact of various coefficients on voltage stability. They utilized self-adaptive control of the droop coefficient to model a VSG and noticed that during disturbances and transient conditions, there was a decrease in frequency and voltage deviation. In [23], a virtual impedance-based control method for VSG was introduced. By utilizing simulated resistivity, the behavior of the VSG was effectively regulated. In [24] proposed fixed parameter damping techniques for VSG control. These techniques incorporated state feedback and a low-pass filter, effectively addressing low-frequency oscillation problems. Notably, these methods also improved the microgrid's ability to attenuate power ripples during operation.

Researchers have developed various approaches to optimize the global maximum power point (GMPP) of PV systems under varying climate conditions, known as maximum power point tracking (MPPT) methods. In reference [25], the researchers introduced MPPT systems that were designed specifically to track the GMPP in the presence of partial shading conditions (PSC). Nevertheless, these algorithms often struggle to accurately identify the true GMPP and can become trapped in local power peaks due to the constant variations in the duty ratio of partial shading conditions (PSC). Consequently, the power output of PV procedures may be reduced [26].

To check the limits associated with typical algorithms, researchers have proposed hybrid MPPT algorithms that leverage the advantages of combining two unlike algorithms. As an example, in [27], an algorithm utilizes large datasets in real-time and employs a filtering mechanism to eliminate unwanted data points was introduced. While the method mentioned above exhibits a rapid response and lower training error, it tends to have fewer bifurcations caused by climatic variations. Similarly, another researcher proposed a hybrid algorithm that combines linear tangent (LT) and interpolation techniques and developed a method to track the GMPP when partial shading conditions (PSC) occur. This algorithm effectively overcomes certain limitations and exhibits a delay in response time under rapidly changing climatic conditions because of the need for re-loading of the DC scheme.

During recent developments, researchers have devised a hybrid approach that combines to achieve high efficiency in PV applications, researchers focused on optimizing multilevel inverters using an (ANN) combined with (NR) algorithm [29]. This method demonstrates efficiency by utilizing the ANN for guiding and estimate purposes, while NR is engaged for additional optimization.

The model and performance assessment of a PV generation method addresses the challenges posed by partial shading conditions. The system involves a DC/DC converter

and a DC/AC inverter, which are essential components for grid addition of PV systems. To enhance energy harvesting capabilities, in the DC/DC converter, a novel MPPT algorithm, inspired by the construction of the Giza Pyramid, is utilized. This Giza Pyramid construction based MPPT algorithm utilizes unique techniques derived from mathematical principles and optimization strategies inspired by the pyramid's design. Its aim is to enhance the overall effectiveness and working of PV systems, particularly in scenarios with partial shading.

The control of the PV technique's inverter is achieved through the utilization of virtual synchronous generation (VSG) control. This control strategy enables the emulation of synchronous generator characteristics, this includes various functionalities such as voltage and frequency regulation, inertia response, and fault ride-through capability. The integration of VSG control allows the PV system to seamlessly connect with existing power grids, maintain grid stability during normal operation, handle grid disturbances, and support grid voltage and frequency control. The study employs MATLAB/Simulink for system simulation, comparing the results with those obtained from a PV system utilizing a Particle Swarm Optimization (PSO) created MPPT algorithm. This comparative analysis provides valuable insights into the performance and efficacy of the aimed Giza Pyramid construction based MPPT algorithm under partial shading conditions. Overall, the research aims to contribute to the advancement of PV generation systems, specifically addressing challenges that are related to partial shading, and offers potential improvements in efficiency, performance, and grid integration capabilities.

2. PV Cell modelling

The PV cell is represented by a two-diode model, illustrated in Figure 1, includes two reverse saturation diodes with diode currents represented by I_{d1} and I_{d2}. The ideality factors of these diodes are denoted by η_1 and η_2, respectively. The presence of an additional second diode current in the model highlights the influence of combined losses occurring in the depletion region of the cell examined.

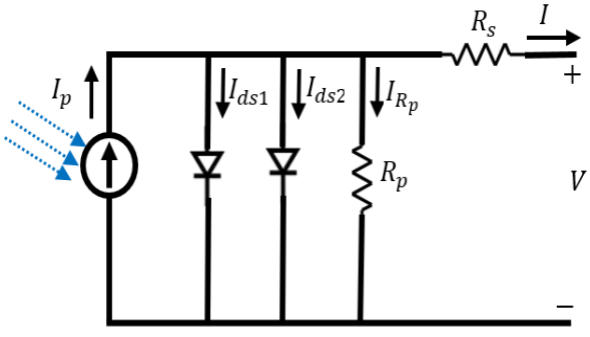

Fig. 1. Equivalent circuit of PV panel with two diodes

Achieving optimal efficiency in a PV generation system necessitates operating at the maximum power point, which is impacted by two atmospheric parameters: irradiation and temperature. In cases where the rated power of a single PV panel is inadequate, Attaining the desired voltage and power output can be accomplished by connecting multiple low-rated panels in either series or parallel configurations. Partial shading of some PV panels, caused by clouds, buildings, or trees, can result in non-uniform irradiance levels, leading to voltage drops across those panels. As a result of this voltage drop, the affected PV panels can exhibit behavior like that of a load on the remaining PV system which causes power and voltage mismatches and potentially leads to hotspot effects. To relieve the effects of partial shading and prevent hotspots, bypass diodes are installed across the PV panels.

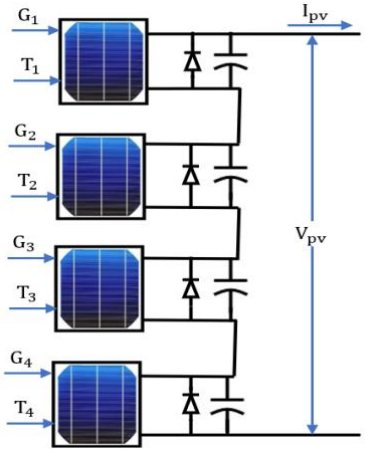

Fig. 2. PV generation system with four series connected PV arrays.

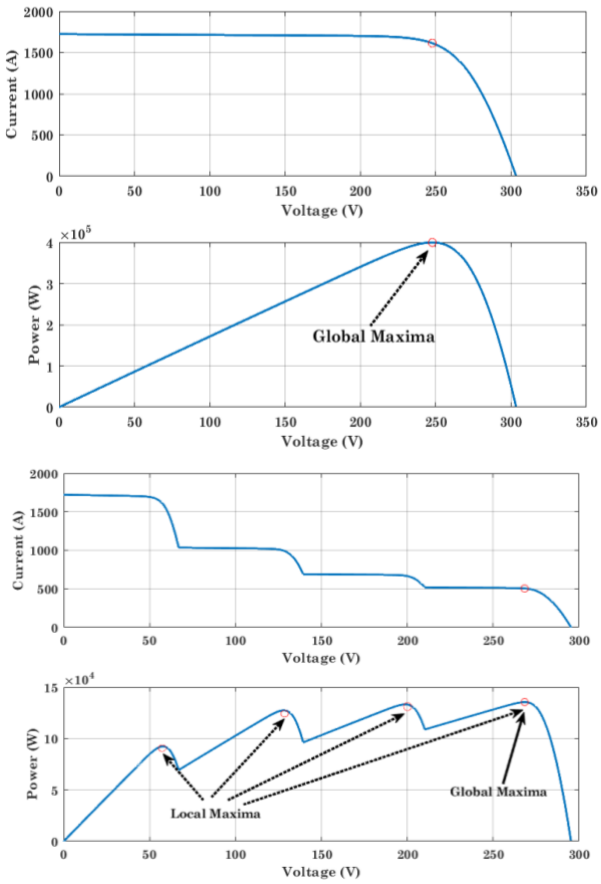

Fig. 3. IV and PV characteristics without and with partial shading condition

Figure 3 illustrates the characteristics of a PV system including the current-voltage (IV) and power-voltage (PV) curves comprising four series-connected PV arrays. It showcases the system's behaviors under both uniform irradiance levels and partial shading conditions. The maximum capacity of each PV array is 100 kW, and the total capacity of the PV system reaches 400 kW at maximum. In situations where the irradiance levels are uneven, the power vs voltage curve of the PV array exhibits multiple local maxima in addition to a single global maximum. To maximize the utilization of solar energy from a PV system, it is key to run the system at the total optimum, even when exposed to non-uniform irradiance conditions. To achieve this goal, the utilization of efficient algorithms and control strategies becomes necessary to continuously track and maintain the PV system at the GMPP. The study utilizes a novel Giza Pyramid Construction (GPC) based MPPT algorithm to efficiently obtain extreme power from the PV generation system.

3. Partial Shading Conditions

When PV module arrays experience partial shading conditions (PSC), their efficiency is significantly reduced because of reduced output voltage and current. PSC can be produced by a variety of factors, this encompasses shading effects caused by dust, nearby structure, clouds, as well as malfunctioning of PV modules. One of the major consequences of PSC is the emergence of multi-power peaks on the P-V curve, namely the local and global power peaks. These peaks indicate that the PV system is producing multiple power outputs, which can further decrease its overall efficiency. The highest power point on the power-voltage (PV) curve is commonly referred to as the global power peak, representing the optimal power output. Conversely, the lowest power peak resulting from abrupt environmental changes is known as the local power peak. To ensure optimal proficiency of the PV system, the utilization of an MPPT controller is needed. The adoption of a novel Giza Pyramid Construction (GPC) based MPPT algorithm enables the PV system to control at its peak efficiency, even when subjected to partial shading conditions (PSC).

3.1. GIZA Pyramid Construction Algorithm

Pseudo-code of proposed algorithm

1. Initialize dimensions of the problem, population size, maximum iterations, and down and high limits of the result
2. Initialize an array with random values.
3. Calculate the cost of each initialized stone block or worker, find the best worker and term him as Pharaoh's agent
4. **While** ite< Maximum iterations **do**
5. **For** i=1 to the number of stone blocks or workers **do**
    1. Determine the stone block displacement (Eq. 10)
    2. Determine the worker movement (Eq. 11)
    3. Find the new position (Eq. 12)
    4. Find the probability of substituting the workers (Eq. 13)
    5. Calculate the next position and cost
    6. **If** cost<Pharaoh's agent cost, **then**
        1. Set worker of new cost is Pharaoh's agent
    7. **End if**
6. **End For**
7. **End While**
8. Solution=c

3.2. Power Quality

High-quality power refers to a consistent voltage supply that operates within a predetermined range. Power quality concerns are focused on deviations from the essential frequency and the presence of a pure sinusoidal waveform in electrical systems. High-quality power is characterized by an alternating current (AC) frequency that closely matches the required frequency and the absence of any distortions in the waveform. These issues can have detrimental effects on the lifespan of electrical devices. Power generation is the capability to consistently generate power at a required frequency, through minimal variations. Power quality problems can have a major effect for consumers, as they can result in lower system power factors and ultimately lead to higher monthly utility bills. Several organizations worldwide are dedicating significant efforts to the development of power quality standards that are met for various electrical equipment.

The emergence of harmonics is considered the most significant power quality issue. Harmonics are characterized by voltages or currents that have frequencies that are integer multiples of the fundamental/intended frequency [31]. When the harmonics align with the intended voltage or current, it can lead to waveform distortion. In grid-integrated PV systems, harmonics can originate from multiple sources, including converters, power electronics devices, and controlled or uncontrolled rectifier loads. These loads can cause fluctuations in current, leading to a distorted waveform and resulting in voltage drops across the system impedance. To measure the level of distortion in the waveform with respect to the fundamental waveform, Researchers often use Total Harmonic Distortion (THD) as a metric for power quality. According to the IEEE-519 standard, in an ideal scenario, a sinusoidal waveform would have a Total Harmonic Distortion (THD) of 0%, it is recommended to maintain the Total Harmonic Distortion (THD) level in an electrical system below 5%. Equations (1) and (2) are widely utilized for calculating the THD level of voltage and current, respectively.

$$THD_V = \frac{\sqrt{\sum_{n=2}^{N} v_n^2}}{v_1} \times 100\% \quad (1)$$

$$THD_1 = \frac{\sqrt{\sum_{n=2}^{N} I_n^2}}{I_1} \times 100\% \quad (2)$$

Equations (1) and (2) determine the THD levels of voltage and current, where V_n and I_n denote the respective nth harmonics of voltage and current. Additionally, V_1 and I_1 represent the base magnitude. The calculation considers the maximum harmonic order (N) for consideration. A high THD level can have a major impact on the power quality and power factor. Equation (3) illustrates the relationship between the power factor and harmonics.

$$PF = \frac{1}{\sqrt{1 + \left(\frac{THD\%}{100}\right)^2}} \quad (3)$$

Other types of frequency disturbances can be characterized by Voltage variations, like unbalanced voltage, voltage sag, swell, and interruption, among others, are characterized by the magnitude of the voltage deviation. These variations can have durations ranging from instantaneous to transient or temporary. The usual description and limits of these voltage modifications are defined by IEEE norms [32].

4. Grid connected PV System Description

Figure 4 depicts the block diagram of a grid-connected PV system, which employs a two-stage system to enable power supply from PV generation to the grid. It incorporates a GPC-based MPPT control, which enables tracking of the GMPP and ensures the maintenance of an ideal voltage across the capacitor of DC link. The PV system remains operational even when abnormal weather conditions are present. The boost converter design is utilized to increase the DC link voltage to the required level for the DC/AC inverter, utilizing the bus capacitor for this purpose. The capacitor between boost converter and the significance of VSC lies in its ability to ensure the generation of a steady DC voltage and it helps in reducing voltage fluctuations across the PV array.

The capacitor positioned between the boost converter and VSC serves several essential functions. These include stabilizing the DC voltage, minimizing voltage ripples, and acting as a power storage system. It plays a crucial role in supplying power to the inverter during transient faults, partial shading conditions (PSC), and similar occurrences. To enhance power quality, the connection between the DC/AC inverter and the utility grid incorporates an LC filter, specifically designed to mitigate high-order harmonics. Additionally, an inverter control loop system is implemented in the setup by regulating the grid-interfacing inverter, enabling the conversion of DC power to AC power.

Under diverse operating conditions, the proposed system demonstrates high efficiency and power quality. To improve power condition by controlling the grid interfacing inverter, a double control loop is employed. The control system contains an inner current loop and an outer voltage loop, which rely on the sensing of the source voltages and VSC output currents. Park's transformation is adopted to convert the currents and voltages into DQ frame. The aim of this transformation is to establish an operating point that guides the PWM (Pulse Width Modulation) to control the IGBT (Insulated Gate Bipolar Transistor) of the inverter, resulting in the production of a smooth sine wave. To achieve this, a dual control loop system is implemented, containing an inner loop for current controller and an outer loop for voltage control. This system monitors the three-phase inverter currents and grid voltages. The presented research paper introduces a grid-integrated PV system that is interconnected with both linear and nonlinear loads. To achieve synchronization between the grid and inverter, the system incorporates the technique of double second-order generalized integrator phase-locked loop (DSOGI-PLL).

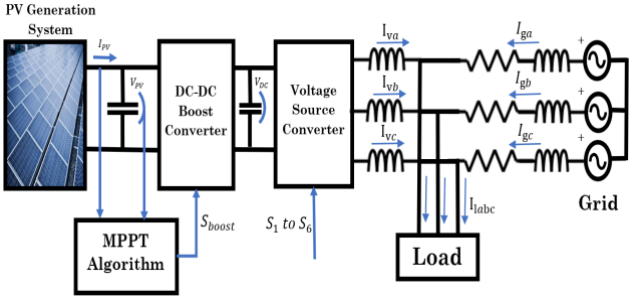

Fig. 4. Grid integrated PV generation System

4.1. VSG-ESS Control Method

The "P-Droop" mechanism is used to control the primary frequency, whereas the "Q-Droop" technique is implemented to regulate the output voltage which is mostly associated with automatic power and the voltage measured at the point of common coupling (PCC). Secondary frequency control employs the inertial equation in VSG. The terminal voltage is significantly influenced by the reactive power supplied by a power generator, which is utilized to simulate the equivalent line inductive impedance between the inverter output and the PCC. The terminal voltage often exhibits a drooping behavior. The swing equation is of utmost importance when evaluating the transient stability of a power system since it enables the examination of power system stability. The swing equation is a mathematical representation of the rotor's movement relative to the stator field over time. It is typically presented in the following form:

$$J\frac{d\omega_m}{dt} = \frac{P_m - P_e}{\omega_m} - D(\omega_m - \omega_o) \quad (4)$$

The swing equation is defined by the relationship between the electromagnetic power (P_e), mechanical power (P_m), and the rated (ω_0) and mechanical (ω_m) angular frequencies. The damping coefficient is represented by D, and the moment of inertia of the virtual rotor is denoted by J. The load bus's voltage and current measurements in three phases undergo a conversion process to DQ representation using Park's transformation. Park's transformation is a mathematical tool that allows for the conversion of three-phase electrical quantities, such as voltage and current, to two-phase dq quantities that are easier to analyze and control.

In addition, the analysis of real and reactive power from the grid serves as input signals for the P-F and Q-V droop control mechanisms. These blocks operate by altering the output frequency and voltage levels of the system in response to changes in load demand. This is achieved by utilizing the power measurements of the grid as a reference for the droop control blocks. Frequency and voltage control of the system were achieved through the implementation of droop controllers. The Q-V droop regulator establishes the reference voltage, while the P-F droop controller determines both the phase angle and frequency of the Virtual Synchronous Generator (VSG).

The droop controllers ensure the system operates consistently and continuously by modifying these parameters in accordance with variations in load demand. The source current for the current control block is calculated using the synchronous approach. After obtaining the source current using the synchronous approach, the current control module computes the necessary three-phase source voltage for implementing Pulse Width Modulation (PWM). Utilizing the reference voltage and the angle produced by the P-F drop controller, the system employs the values to fulfill its operational requirements. The PWM module generates gate pulses that are transmitted to the inverter. The gate pulses facilitate the inverter in delivering the necessary real and reactive power to meet the load demand. The primary purpose of the LC filter is to reduce or eliminate the output harmonics generated by the inverter.

4.2. Active Power-Frequency Control

P-F and Q-V droop controls are widely employed as preferred methods in medium and high voltage microgrids with distributed generation systems to effectively handle variations in real and reactive power. By modifying the frequency and voltage levels of the system output in accordance with load demand fluctuations, these control methods ensure the stable operation of the microgrid. By using P-F and Q-V droop controls, the distributed generation system can effectively manage the balance between real and reactive power, ensuring reliable and efficient operation of the microgrid.

$$P_m = P_{ref} + k_w(\omega_{ref} - \omega_g) \quad (5)$$

P_{ref} is the required active power to be injected by the inverter, ω_{ref}, and ω_g are reference and actual angular frequencies, k_w is the active power droop measurement.

4.3. Reactive Power-Voltage Control

The voltage converted by a VSC commonly exhibits a characteristic of decreasing or drooping behavior in relation to reactive power. This drooping behavior is closely associated with the reactive power produced by the inverters.

$$V_{ref} = V_{nom} - k_q(Q_{ref} - Q_{inv}) \quad (6)$$

V_{nom} rated voltage, Q_{ref} is the reference reactive power to be injected by the inverter, Q_{inv} actual inverter output reactive power, k_q is the reactive power droop coefficient, V_{ref} reference voltage at the output of the inverter.

The swing equation for virtual synchronous generator-based inverter control is given as

$$P_m - P_{inv} = J_s\omega_g \frac{d\omega_g}{dt} + D_p(\omega_{ref} - \omega_g) \quad (7)$$

D_p virtual damping factor, J_s is the virtual inertia, P_m virtual shaft real power.

From the equation (1), θ_g can be calculated as

$$\theta_g = \int \omega_g = \int \left\{ \int \frac{1}{J_s\omega_g} \left[(P_m - P_{inv}) - D_p(\omega_{ref} - \omega_g) \right] dt \right\} dt \quad (8)$$

For reactive power control, virtual electromotive force V_{ma}, V_{mb} and V_{mc} are calculated as

$$\left.\begin{aligned} V_{ma} &= \psi_f \omega_g \sin(\theta_g) \\ V_{mb} &= \psi_f \omega_g \sin\left(\theta_g - \frac{2\pi}{3}\right) \\ V_{mc} &= \psi_f \omega_g \sin\left(\theta_g + \frac{2\pi}{3}\right) \end{aligned}\right\} \quad (9)$$

Ψ_f is the virtual rotor flux which regulates the actual voltage magnitude V_{mag} to V_{ref} generated by reactive power droop control. Error between V_{mag} and V_{ref} is the input to the PI controller and output of the PI regulator is adopted as virtual rotor flux ψ_f. Before calculating virtual electromotive force, high frequency components in virtual rotor flux are filtered by low pass filter. Inner current control and outer voltage and active power regulator are adopted to generate reference voltages V_{aref}, V_{bref} and V_{cref} for inverter. By applying sinusoidal pulse width modulation on these reference voltages, switching pulses required by inverter can be generated.

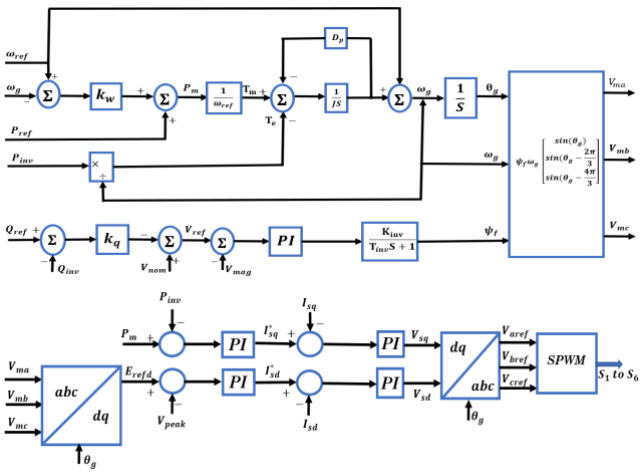

Fig. 5. Virtual synchronous generator base control strategy for Inverter

5. Simulation results

The GPC based MPPT for DC-DC converter and discrete VSG based control system for DC-AC inverter are verified through four case studies using MATLAB/SIMULINK. The PV system contains four series-

connected PV arrays, and each array comprises 80 parallel strings and 5 modules linked in series per string.

5.1. Case 1.

In Case Study 1, the presentation of the proposed Giza Pyramid Construction (GPC)-based MPPT technique is examined in partial shading conditions (PSC). The study examines variations in solar irradiance, with different levels measured at 1000 W/m^2, 600 W/m^2, 400 W/m^2, and 800 W/m^2, while the module temperature fluctuates between 35°C, 29°C, 21°C, and 30°C. To maintain a consistent DC current within defined boundaries for the inverter and enhance its responsiveness, the DC link inductor is set up with a frequency of 100 mH, the proposed discrete VSG control system is evaluated with a linear load of 400 kW and in terms of voltage and current total harmonic distortion (THD) as well as active and reactive power, the value of 100 kVAR is being evaluated. The comparison involves evaluating the proposed GPC MPPT and discrete VSG inverter control strategy in contrast to the PSO MPPT technique.

Table 1. Pattern 1 of Irradiance values in W/m^2 for case 1

	0 to 2 sec	2 to 4 sec	4 to 6 sec	6 to 8 sec
PV Array 1	1000	600	400	800
PV Array 2	1000	600	400	800
PV Array 3	1000	600	400	800
PV Array 4	1000	600	400	800

During Case Study 1, the MPPT method built on GPC showcased accurate tracking of the maximum PV power corresponding to variations in irradiance. As a result, the system achieved an outstanding efficiency level of 99.85% and exhibited remarkably minimal energy losses, measuring just 0.15%. The suggested MPPT technique successfully upheld a consistent optimal DC link voltage for the input side of the inverter, while the Boost DC-DC converter maintained a constant switching frequency of 10 kHz. Notably, the aimed method demonstrated rapid tracking capabilities, accurately identifying the true GMPP within a mere 0.04 seconds.

Figure 6 illustrates the PV generation system's inverter output voltage and current. At 1 second, a decrease in the PV generated power resulted in a reduction in the inverter's output current. FFT analysis revealed that the inverter output current exhibited a total harmonic distortion (THD) of 1.32% when using the proposed GPC-based MPPT. However, when employing the PSO-based MPPT, the current THD increased to 3.4% due to higher ripples in the DC side current.

During the grid THD analysis, it was noted that the grid current waveform spectrum exhibited prominent harmonics primarily at the third and fifth orders. Consequently, the designed inverter control system was specifically crafted and optimized to reduce the presence of these harmonics at their individual frequencies. Figure 7 depicts the inverter voltage and current waveforms after filtering, showcasing the effectiveness of the applied measures. The load voltage and current profiles are depicted in Figure 8. The inverter's power profiles, both in terms of dynamics and reactive components obtained using GPC MPPT (Figure 9) and PSO MPPT (Figure 10), are presented. It is evident that the transient behavior of the power profiles with GPC MPPT is superior to that of PSO MPPT, particularly during changes in irradiance. Figure 11 and Figure 12 depict the dynamic and fluctuating power of the load using GPC MPPT and PSO MPPT techniques, respectively. Additionally, Figure 13 and Figure 14 present graphical illustrations depicting the injection of active and reactive power into the grid.

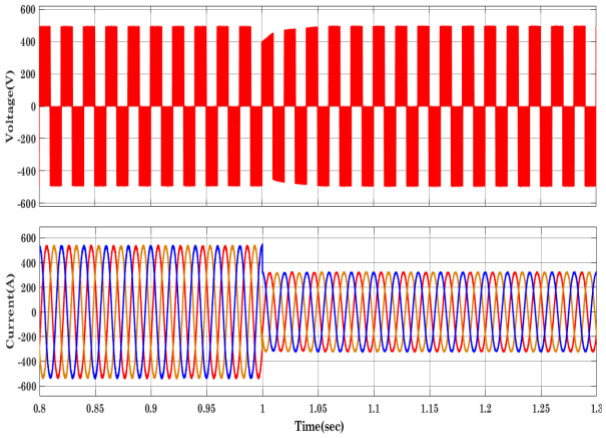

Fig. 6. PV Inverter output voltage and current

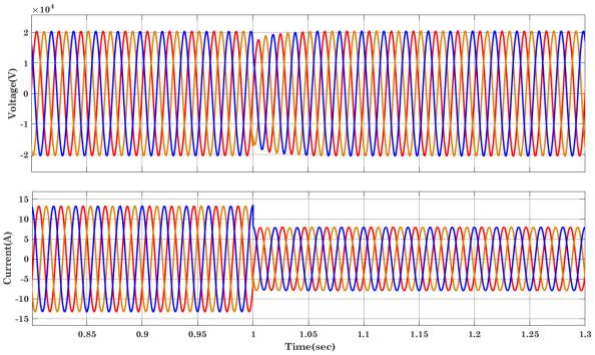

Fig. 7. Inverter output voltage and current after filtering

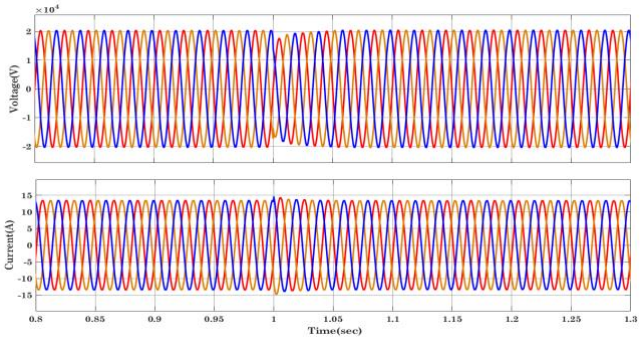

Fig. 8. Load Voltage and Current

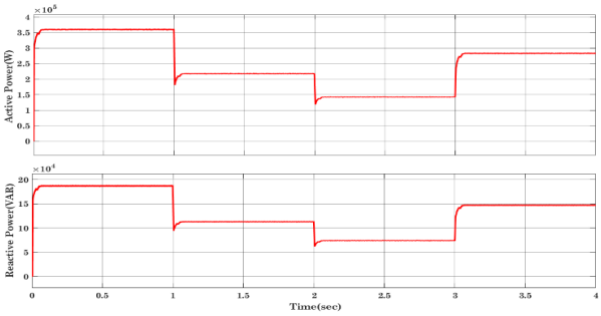

Fig. 9. Inverter Output active and reactive power with GPC MPPT

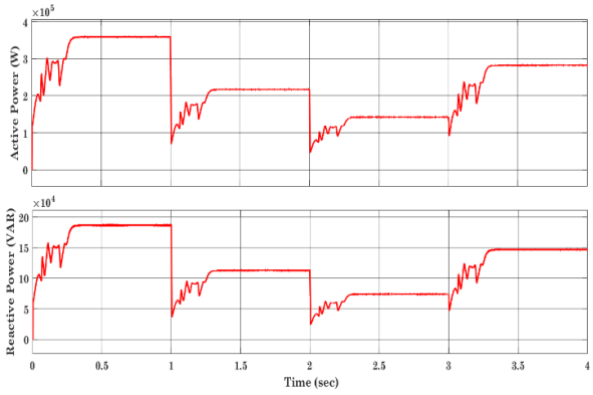

Fig. 10. Inverter Output active and reactive power with PSO MPPT

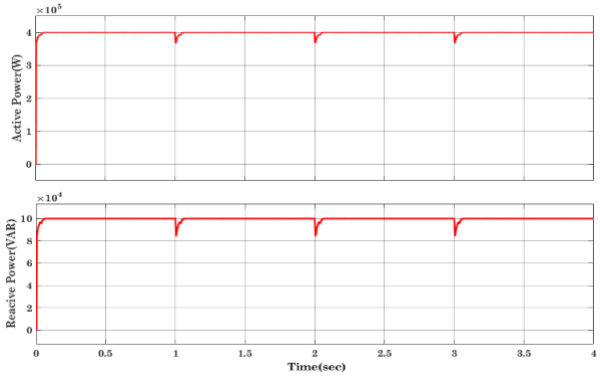

Fig. 11. Load Active and Reactive Power with GPC MPPT

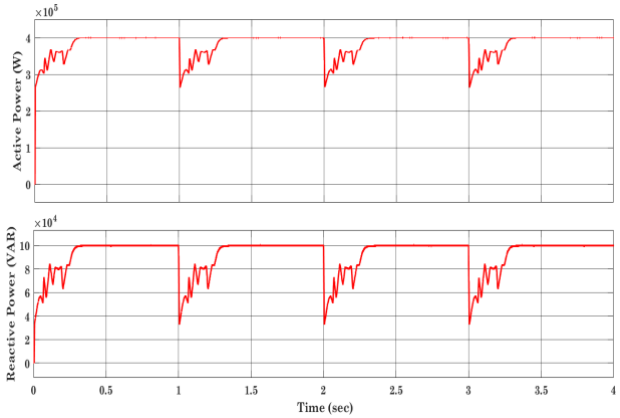

Fig. 12. Load Active and Reactive Power with PSO MPPT

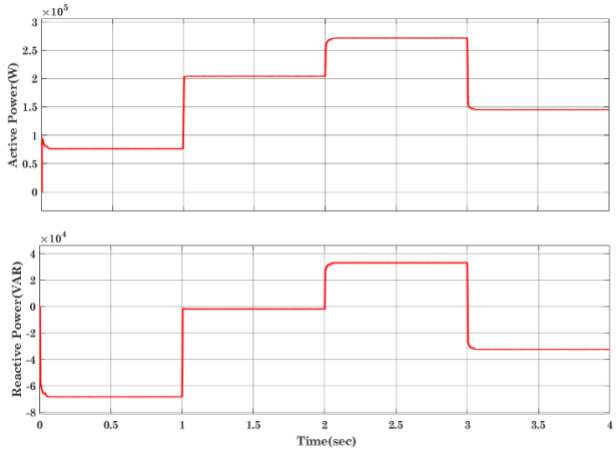

Fig. 13. Grid Active and Reactive Power with GPC MPPT

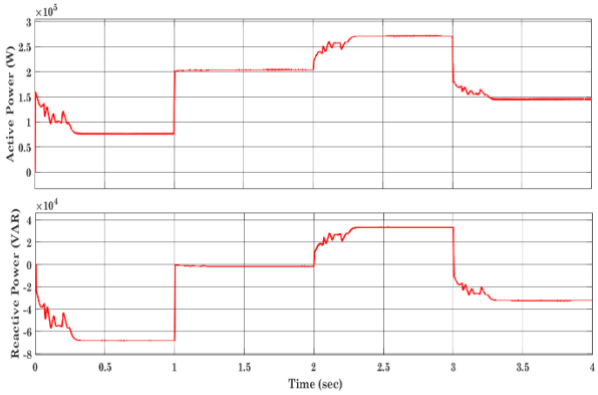

Fig. 14. Grid Active and Reactive Power with PSO MPPT

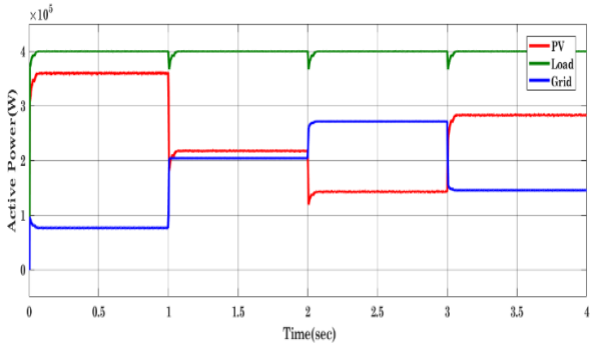

Fig. 15. PV, Load and Grid Active Power with GPC MPPT

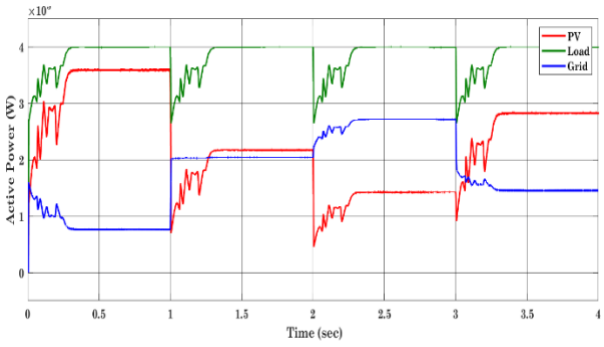

Fig. 16. PV, Load and Grid Active Power with PSO MPPT

5.2. Case 2.

Case study 2 evaluates the efficacy of the GPC-based MPPT and discrete VSG control system under partial shading conditions. The study involves varying solar irradiance levels and module temperature changes to estimate the execution of the system. The solar irradiance levels used in the study are 1000 W/m^2, 650 W/m^2, and 930 W/m^2 for PV1, 1000 W/m^2, 300 W/m^2, and 380 W/m^2 for PV2, 1000 W/m^2, 450 W/m^2, and 250 W/m^2 for PV3, and 1000 W/m^2, 720 W/m^2, and 550 W/m^2 for PV4. The module temperature changes used in the study are 35°C, 25°C, and 28°C. To minimize system losses, the DC link inductor is decreased to a value of 80 mH. A constant linear resistant load of 200 kW is linked to the system. The THD is analyzed using the Fast Fourier Transform (FFT) technique in unity with the IEEE 519 standard.

Figure 17 displays the voltage and current output of the PV inverter. However, there are harmonics exhibits in the voltage signal. To mitigate these harmonics, an inductive filter is employed, and Figure 18 portrays the filtered voltage and current that ensued. The load voltage and current waveforms are presented in Figure 19. Figure 20 presents the active and reactive power profiles of the PV inverter, while Figure 21 showcases the power profiles of the load. Figure 22 illustrates the power profiles of the grid. The grid shows an important task in maintaining uninterrupted power supply to the load, particularly in scenarios where there is a decrease in irradiance due to partial shading. During such circumstancesThe grid functions as an alternative power source, providing compensation for the decreased power generation from the PV system.

By providing the further power needed by the load, the grid ensures a consistent power supply to meet the load requirements, thereby guaranteeing the reliability and continuity of electrical supply in challenging conditions.

Table 2. Pattern 2 for irradiance values in W/m^2 for case 2

	0 to 2 sec	2 to 4 sec	4 to 6 sec
PV Array 1	1000	650	930
PV Array 2	1000	300	380
PV Array 3	1000	450	250
PV Array 4	1000	720	550

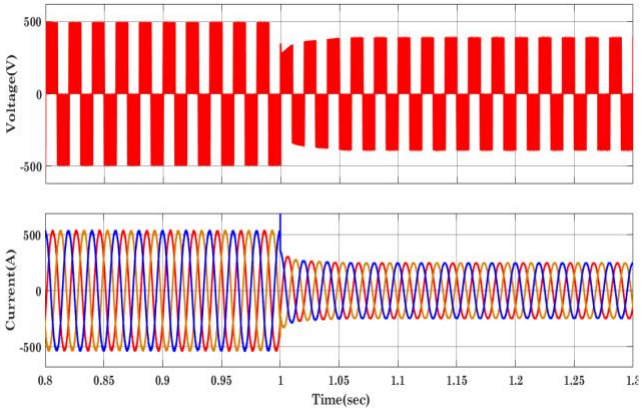

Fig. 17. Inverter Output Voltage and Current

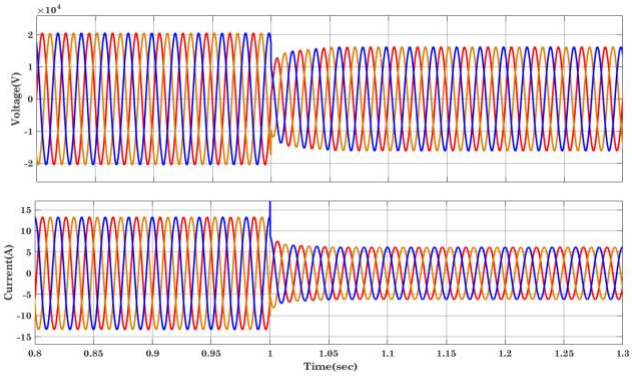

Fig. 18. Inverter output Voltage and Current after filtering

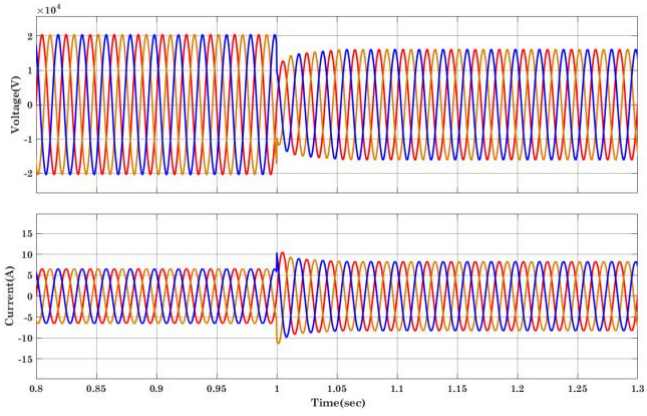

Fig. 19. Load Voltage and Current

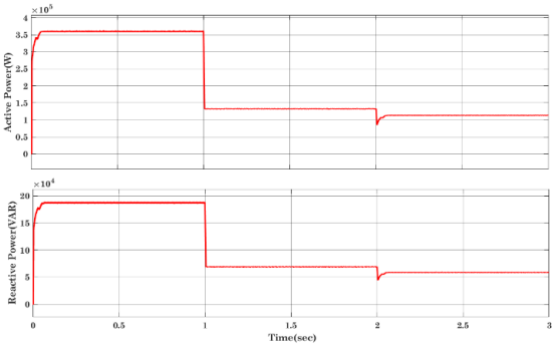

Fig. 20. Inverter Active and Reactive Power

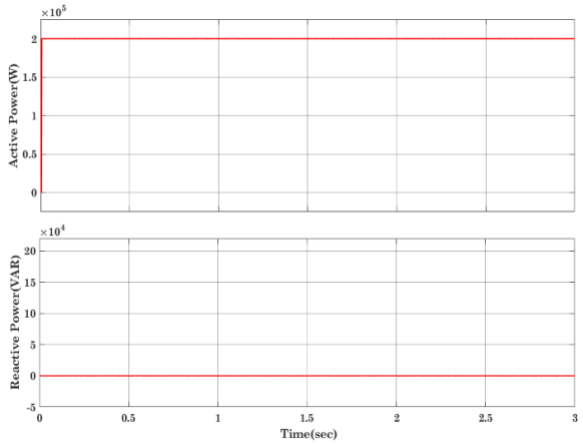

Fig. 21. Load Active and Reactive Power

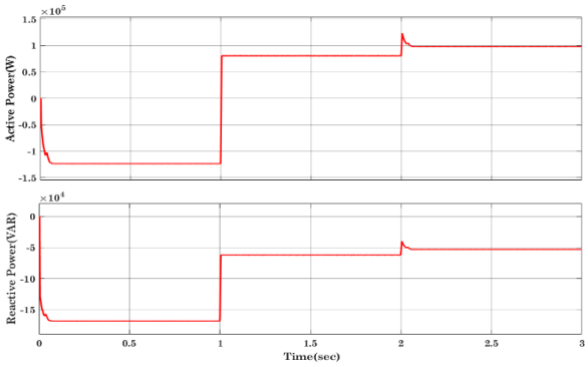

Fig. 22. Grid Injected Active and Reactive Power

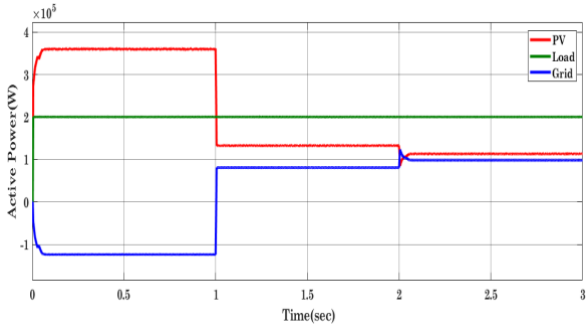

Fig. 23. PV, Load and Grid Active Power

5.3. Case 3.

Case study 3 evaluates the proposed MPPT and inverter control strategy under the worst partial shaded irradiance pattern. In this array, the third PV array receives 0 irradiance, which signifies the failure of the PV array. A bypass diode across the respective PV array short circuits it for continuous working of the PV system. The study aims to enhance power quality in such conditions. To reduce system losses, the inductor in DC link is lowered to 50 mH. The proposed discrete VSG control system was evaluated with a linear load of 400 kW and 100 kVAR. Figure 24 displays the voltage and current output produced by the PV inverter. However, there are harmonics existent in the voltage signal. To mitigate these harmonics, an inductive filter is employed, and the resulting filtered voltage and current are depicted in Figure 25. The load voltage and current waveforms are presented in Figure 26. The (THD) of the load current is measured to be 1.3%, indicating a relatively low level of harmonic content.

Figure 27 represents the active and reactive power profiles of the PV inverter, while Figure 28 illustrates the power profiles of the load. Figure 29 showcases the power profiles of the grid. To ensure uninterrupted power supply to the load, especially during situations where there is a reduction in irradiance due to partial shading conditions or there is a failure in any PV array, the grid plays a crucial role. It can handle the additional power required by the load, compensating for the decrease in power generated by the PV system. This ensures a constant power supply to meet the load requirements, even under challenging conditions.

Table 3. Pattern 3 for irradiance values in W/m^2 for case 3

	0 to 2 sec	2 to 4 sec	4 to 6 sec
PV Array 1	1000	650	930
PV Array 2	1000	300	380
PV Array 3	0	0	0
PV Array 4	1000	720	550

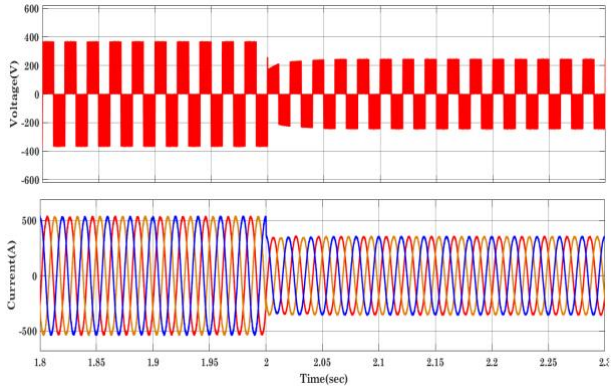

Fig. 24. Inverter Voltage and Current

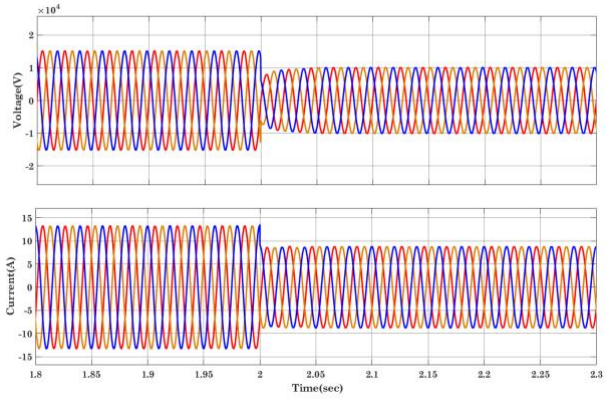

Fig. 25. Bus B1 Voltage and Current

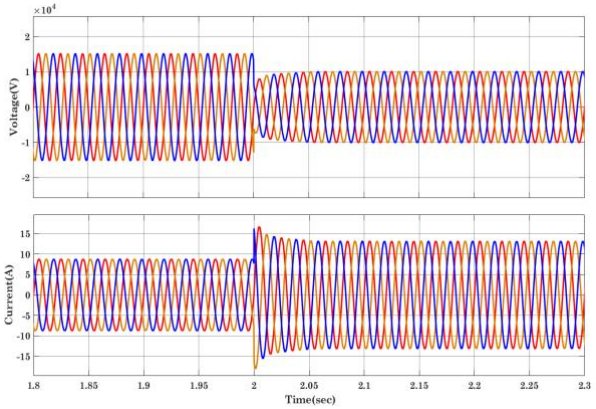

Fig. 26. Load Voltage and Current

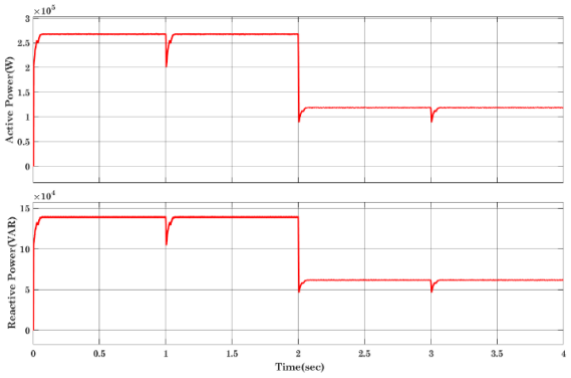

Fig. 27. Inverter output Active and Reactive Power

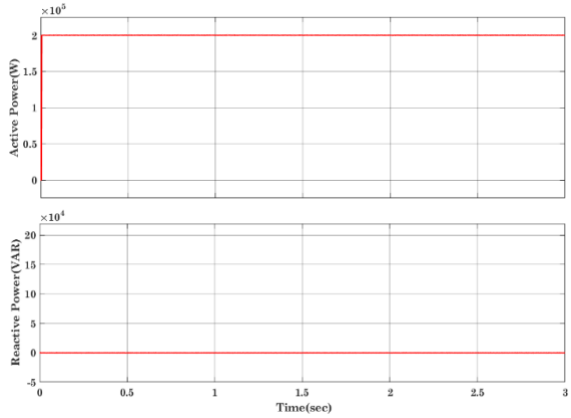

Fig. 28. Load Active and Reactive Power

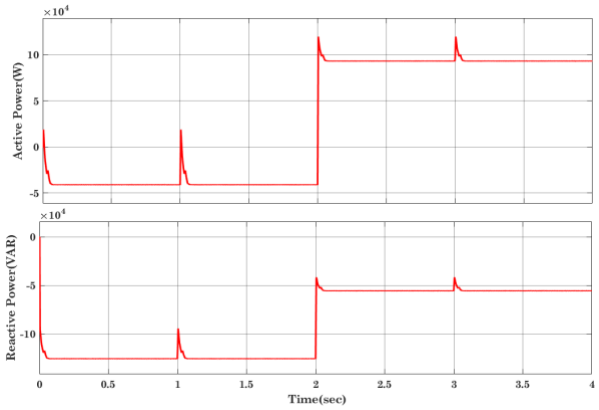

Fig. 29. Grid Injected Active and Reactive Power

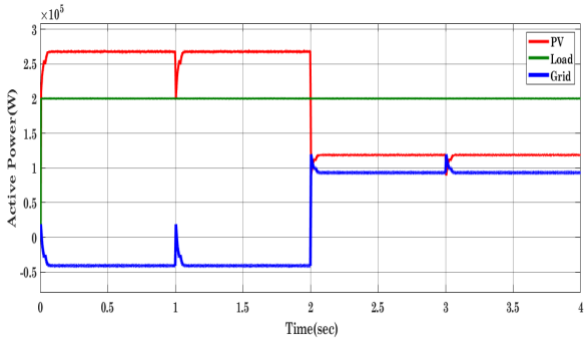

Fig. 30. PV, Load and Grid Active Power

5.4. Case 4

Case study 4 evaluates the proposed work for irradiance values of a 24-hour day, gathered from the National Renewable Energy Laboratory (NREL) [33]. Fig 31 presents variable irradiance values. A consistent linear load with a power demand of 400 kW and a reactive power demand of 100 kVAR is connected and the results are examined to check the constant power provided to the load. The power output of the solar PV system is determined by utilizing the provided irradiance values. To ensure the system meets the load requirements, the power output from the PV system and the grid are interconnected with the load demand. This case demonstrates the feasibility of the offered work for different irradiance values. Fig 32 depicts load active power, PV inverter active power and grid active power. The outcome shows that the system can meet the load requirements for a 24-hour period, even with a constant linear load. This suggests that the system could be used to provide continuous power to a variety of loads.

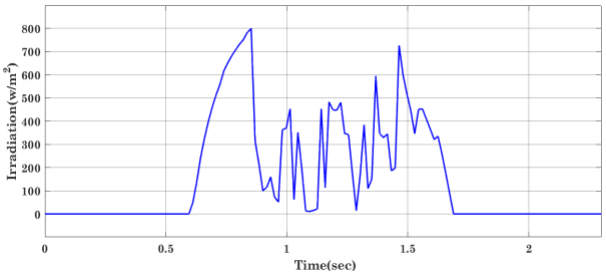

Fig. 31. Variable Irradiance

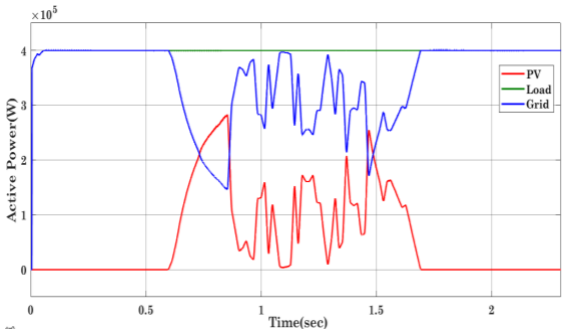

Fig. 32. PV, Load and Grid Active Power

6. Conclusion

This paper presented a complete study on a PV generation system designed to address partial shading

conditions. The system employed a DC/DC converter utilizing a novel MPPT algorithm inspired by the construction of the Giza Pyramid. This algorithm incorporated unique techniques based on mathematical principles and optimization strategies derived from the pyramid's design, enhancing the system's energy harvesting capabilities and overall efficiency. Furthermore, the PV system was controlled by virtual synchronous generation (VSG) controller, which emulated the activities of a synchronous generator. This control strategy enabled seamless integration with the grid by adjusting voltage and frequency, responding to grid disturbances, and supporting grid stability. The utilization of VSG control facilitated reliable and stable power delivery to the grid, even in challenging operational conditions. Simulation of the PV system was conducted utilizing MATLAB/Simulink, and the outcome were associated among those obtained from a PV system utilizing a (PSO) based MPPT algorithm. This comparative analysis provided valuable insights into the performance and efficacy of the future Giza Pyramid construction based MPPT algorithm in handling partial shading conditions. Overall, the findings of this study highlight the potential of the Giza Pyramid construction based MPPT algorithm and VSG control in improving the efficiency, reliability, and grid integration capabilities of PV generation systems. The research contributes to the development of advanced techniques for maximizing PV system performance, particularly in scenarios involving partial shading conditions.

References

[1] Y. M. Atwa, E. F. El-Saadany, M. M. A. Salama, and R. Seethapathy, 2009. Optimal renewable resources mix for distribution system energy loss minimization. IEEE Transactions on Power Systems, 25(1), pp.360-370.

[2] A. J. Roscoe, M. Yu, M., R. Ierna, J. Zhu, A. Dyśko, H. Urdal, and C. Booth, 2016, November. A VSM (virtual synchronous machine) converter control model suitable for RMS studies for resolving system operator/owner challenges. In 15th Wind Integration Workshop.

[3] Akagi, Hirofumi, and Hikaru Sato. "Control and performance of a doubly fed induction machine intended for a flywheel energy storage system." IEEE Transactions on Power Electronics 17, no. 1 (2002): 109-116.

[4] Liu, Ju, Jinyu Wen, Wei Yao, and Yao Long. "Solution to short-term frequency response of wind farms by using energy storage systems." IET Renewable Power Generation 10, no. 5 (2016): 669-678.

[5] Yazdani, Sara, Mehdi Ferdowsi, Masoud Davari, and Pourya Shamsi. "Advanced current-limiting and power-sharing control in a PV-based grid-forming inverter under unbalanced grid conditions." IEEE Journal of Emerging and Selected Topics in Power Electronics 8, no. 2 (2019): 1084-1096.

[6] Rehman, Haseeb Ur, Xiangwu Yan, Mohamed Abdelkarim Abdelbaky, Mishkat Ullah Jan, and Sheeraz Iqbal. "An advanced virtual synchronous generator control technique for frequency regulation of grid-connected PV system." International Journal of Electrical Power & Energy Systems 125 (2021): 106440.

[7] J. Liu, Y. Miura, H. Bevrani, T. Ise, Enhanced virtual synchronous generator control for parallel inverters in microgrids. IEEE Transactions on Smart Grid. 2016 Feb 8;8(5):2268-77.

[8] G. Denis, T. Prevost, P. Panciatici, X. Kestelyn, F. Colas, and X. Guillaud, 2015, July, Review of potential strategies for transmission grid operations based on power electronics interfaced voltage sources. In 2015 IEEE Power & Energy Society General Meeting (pp. 1-5). IEEE.

[9] A. Muhtadi, D. Pandit, N. Nguyen, and J. Mitra, 2021, Distributed energy resources based microgrid: Review of architecture, control, and reliability. IEEE Transactions on Industry Applications, 57(3), pp.2223-2235.

[10] M. A. Useche Arteaga, 2020. Integration of photovoltaic solar generation systems with energy storage for improving electric power quality.

[11] J. Alipoor, Y. Miura, and T. Ise, 2014, Power system stabilization using virtual synchronous generator with alternating moment of inertia. IEEE journal of Emerging and selected topics in power electronics, 3(2), pp.451-458.

[12] X. Liang, C. Andalib-Bin-Karim, W. Li, M. Mitolo, M. N. Shabbir, Adaptive virtual impedance-based reactive power sharing in virtual synchronous generator controlled microgrids. IEEE Transactions on Industry Applications. 2020 Nov 19;57(1):46-60.

[13] H. Bevrani, T. Ise, and Y. Miura, 2014. Virtual synchronous generators: A survey and new perspectives. International Journal of Electrical Power & Energy Systems, 54, pp.244-254.

[14] S. I. A. Haroon, J. Qian, Y. Zeng, Y. Zou, & D. Tian, (2022). Extended State Observer Based-Backstepping Control for Virtual Synchronous Generator. Electronics, 11(19), 2988.

[15] T. Santhoshkumar, & V. Senthilkumar, (2020). Transient and small signal stability improvement in microgrid using AWOALO with virtual synchronous generator control scheme. ISA transactions, 104, 233-244.

[16] Ferraz, JULIO CR, N. E. L. S. O. N. Martins, and GLAUCO N. Taranto. "Simultaneous partial pole placement for power system oscillation damping control." In 2001 IEEE Power Engineering Society Winter Meeting. Conference Proceedings (Cat. No. 01CH37194), vol. 3, pp. 1154-1159. IEEE, 2001.

[17] Qi, Gongxin, Alian Chen, and Jie Chen. "Improved control strategy of interlinking converters with synchronous generator characteristic in islanded hybrid AC/DC microgrid." CPSS transactions on power electronics and applications 2, no. 2 (2017): 149-158.

[18] J. F. Mushi, K. Han, G. Chen, and J. Daozhuo, 2009, April. Design and implementation of wind turbine imitation system for direct drive permanent magnet synchronous generator using DC motor. In 2009 International Conference on Sustainable Power Generation and Supply (pp. 1-6). IEEE.

[19] Z. H. Zhao, 2022. Improved fuzzy logic control-based energy management strategy for hybrid power system of FC/PV/battery/SC on tourist ship. International Journal of Hydrogen Energy, 47(16), pp.9719-9734.

[20] Liang, Xiaodong, "Adaptive virtual impedance-based reactive power sharing in virtual synchronous generator controlled microgrids." IEEE Transactions on Industry Applications 57.1 (2020): 46-60.

[21] Molina, Marcelo Gustavo, and Pedro Enrique Mercado. "Power flow stabilization and control of microgrid with wind generation by superconducting magnetic energy storage." IEEE Transactions on Power Electronics 26, no. 3 (2010): 910-922.

[22] Cheng, Huijie, Wen Huang, Chao Shen, Yelun Peng, Zhikang Shuai, and Z. John Shen. "Transient voltage stability of paralleled synchronous and virtual synchronous generators with induction motor loads." IEEE Transactions on Smart Grid 12, no. 6 (2021): 4983-4999.

[23] Meyer, Eric, Zhiliang Zhang, and Yan-Fei Liu. "An optimal control method for buck converters using a practical capacitor charge balance technique." IEEE Transactions on Power Electronics 23, no. 4 (2008): 1802-1812.

[24] Li, Tianyang, Buying Wen, and Huaiyuan Wang. "A self-adaptive damping control strategy of virtual synchronous generator to improve frequency stability." Processes 8, no. 3 (2020): 291.

[25] Tamilselvi Selvaraj, Rama Subbu Rengaraj, Giri Rajan babu Venkata Krishnan, Soundhariya Ganesan Soundararajan, Karuppiah Natarajan, Praveen Kumar Balachandran , Prince Winston David, and Shitharth Selvarajan, “Environmental Fault Diagnosis of Solar Panels Using Solar Thermal Images in Multiple Convolutional Neural Networks”, International Transactions on Electrical Energy Systems, Volume 2022, Article ID 2872925, 16 pages https://doi.org/10.1155/2022/2872925Bollipo, Ratnakar Babu, Suresh Mikkili, and Praveen Kumar Bonthagorla. "Critical review on PV MPPT techniques: classical, intelligent and optimisation." IET Renewable Power Generation 14, no. 9 (2020): 1433-1452.

[26] Karuppiah Natarajan, B. Praveen Kumar, Vankadara Sampath Kumar, “Fault Detection of Solar system using SVM and Thermal Image Processing”, International Journal of Renewable Energy Research, Vol. 10, no. 2, June 2020, pp. 1-11, https://doi.org/10.20508/ijrer.v10i2.10775.g7963

[27] Elahi, M., Ashraf, H.M. and Kim, C.H., 2022. An improved partial shading detection strategy based on chimp optimization algorithm to find global maximum power point of solar array system. Energies, 15(4), p.1549.

[28] M. S. Nkambule, A. N. Hasan, A. Ali, and T. Shongwe, 2022. A Novel Control Strategy in Grid-Integrated Photovoltaic System for Power Quality Enhancement. Energies, 15(15), p.5645.

[29] Ebrahimnejad, Sadoullah, and Sasan Harifi. "An optimized evacuation model with compatibility constraints in the context of disability: an ancient-inspired Giza Pyramids Construction metaheuristic approach." Applied Intelligence 52.13 (2022): 15040-15073.

[30] W. A. A. Salem, "Grid connected photovoltaic system impression on power quality of low voltage distribution system." Cogent Engineering 9.1 (2022): 2044576.

[31] Z. Djokic, Sasa, Kurt Stockman, J. V. Milanovic, J. J. M. Desmet, and Ronnie Belmans. "Sensitivity of AC adjustable speed drives to voltage sags and short interruptions." IEEE Transactions on Power Delivery 20, no. 1 (2005): 494-505.

[32] https://nsrdb.nrel.gov/data-viewer